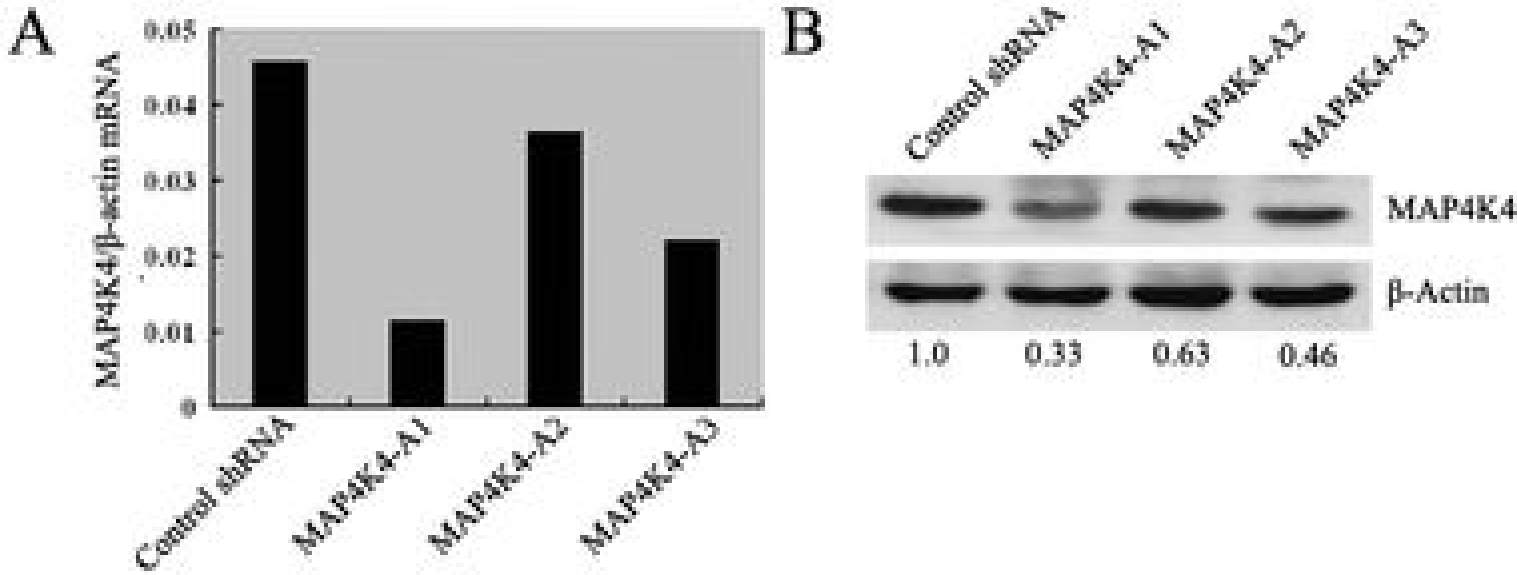
A
MAP4K4/β-actin mRNA
0.05
0.04
0.03
0.02
0.01
0
Control shRNA
MAP4K4-A1
MAP4K4-A2
MAP4K4-A3
B
Control shRNA
MAP4K4-A1
MAP4K4-A2
MAP4K4-A3
MAP4K4
β-Actin
1.0
0.33
0.63
0.46

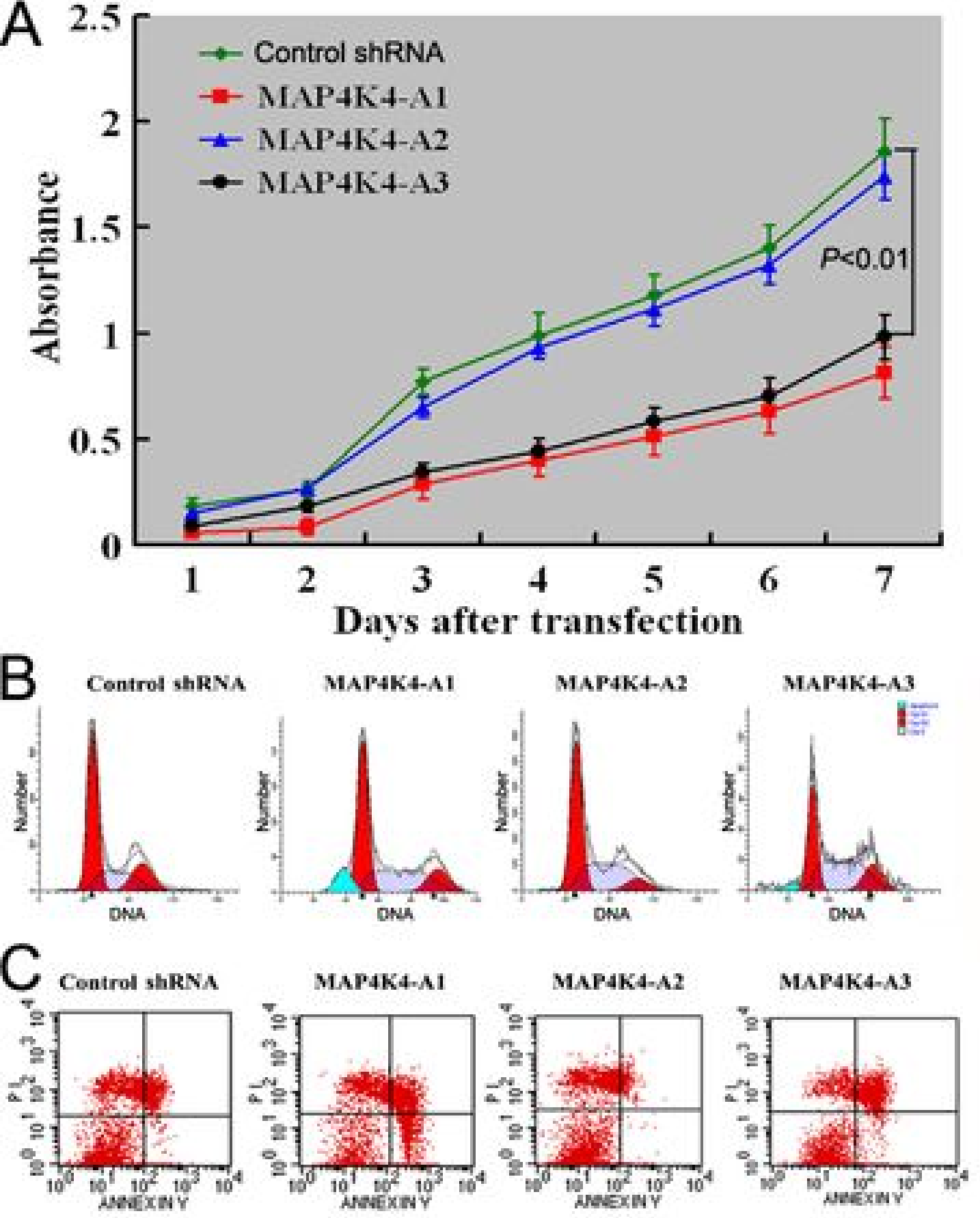
A
Control shRNA
MAP4K4-A1
MAP4K4-A2
MAP4K4-A3
P<0.01
Absorbance
Days after transfection
B
Control shRNA
MAP4K4-A1
MAP4K4-A2
MAP4K4-A3
Number
DNA
C
Control shRNA
MAP4K4-A1
MAP4K4-A2
MAP4K4-A3
ANNEXIN V

Supplementary Figure Legends

Supplementary Fig. 1. Downregulation of endogenous MAP4K4 expression in HepG2 cells by specific shRNAs. qRT-PCR and Western blot analyses of the MAP4K4 mRNA (***A***) and protein (***B***) expression in HepG2 cells stably expressing indicated shRNA plasmids. The values below representative Western bands in *B* indicate the relative MAP4K4 protein levels normalized to β-actin.

Supplementary Fig. 2. ShRNA-mediated silencing of MAP4K4 in Hep3B cells. Hep3B cells at approximately 60% confluence were transiently transfected with MAP4K4-shRNAs (MAP4K4-A1, -A2, and -A3) or control shRNA using Lipofectamine 2000. ***A***, Assessment of cell proliferation by the MTT assay. Hep3B cells expressing MAP4K4-A1 or MAP4K4-A3 shRNAs showed a significantly ($P<0.01$) lower proliferation rate compared to those harboring MAP4K4-A2 or scrambled control shRNAs. $n=6$; error bars, SD. ***B***, Analysis of cell cycle distribution of Hep3B cells expressing indicated shRNAs. Representative flow cytometry histograms of PI-stained cells are demonstrated. ***C***, Representative flow cytometry dot plots of Hep3B cells expressing indicated shRNAs. Early apoptotic cells (Annexin V-FITC positive, PI negative) were increased in MAP4K4-A1- and MAP4K4-A3-producing cells compared to MAP4K4-A2 or control transfectants.

Supplementary Methods

Cell culture. Four human HCC cell lines HepG2, Huh 7, Hep3B, and SMMU-7721 were purchased from Institute of Cellular Research, Chinese Academy of Science (Shanghai, China) and were cultured in Dulbecco's modified Eagle's medium (DMEM) with 10% fetal bovine serum (Gibco BRL, Carpinteria, CA, USA), 50U/ml penicillin, and 50 mg/ml streptomycin in a 5% CO_2 incubator at 37°C.

Generation of stable shRNA-expressing clones. Three shRNAs targeting different regions of the *MAP4K4* transcript were designed following the rules of Tuschl T (1), and their sense sequences were as follows: MAP4K4-A1, 5'-GGGAAGGTCTATCCTCTTATCAAGAGTAAGAGGATAGACCTTCCC-3'; MAP4K4-A2, 5'-GCAGCAGTCAGGTTTATTTCATCAAGAGTGAAATAAACCTGACTGCTGC -3'; and MAP4K4-A3, 5'-GCGGAGAAATACGTTCATAGGTCAAGAGCCTATGAACGTATTTCTCCGC -3'. A negative scrambled control shRNA was purchased from Santa Cruz Biotechnology (sc-108060; Santa Cruz, CA, USA). The shRNAs were separately cloned into pSilencer-2.1-U6 vector (GenScript, Piscataway, NJ, USA), and the resultant constructs (pSilencer-2.1-A1, -A2 and -A3) were verified by DNA sequencing by Shanghai Invitrogen Biotechnology Company (Shanghai, China). For generation of stable transfectants, HepG2 and Hep3B cells at 70-80% confluence

were separately transfected with pSilencer-2.1-A1, -A2 or -A3 using Lipofectamine 2000 (Invitrogen) according to the manufacturer's instructions. After 48 h of transfection, cells were cultured in selection medium containing G418 (400 μg/ml) for 14 days. G418-resistant colonies transfected with the same shRNA were pooled together, and 3 stable cell pools for each of the two HCC cell lines were finally obtained, expressing MAP4K4-A1, -A2 and -A3, respectively. Stable transfectants expressing the scrambled control shRNA were generated similarly. The expression of endogenous MAP4K4 was determined by qRT-PCR and western blot analyses.

Proliferation assay. Cell proliferation was analyzed by a modified tetrazolium salt (MTT) assay (2). HepG2 and Hep3B cells stably transfected with shRNAs or empty vector were separately seeded at a density of 1.5×10^3 cells per well in 96-well microplates, and harvested daily for up to 7 days. The number of viable cells was determined using Cell Titer 96 Non-Radioactive Cell Proliferation Assay (Promega, Madison, WI, USA) according to the manufacturer's protocol. The reduced MTT product was dissolved in 2% dimethylsulfoxide, and the absorbance at 570 nm was measured on a Bio-Rad Microplate Reader (Bio-Rad, Hercules, CA). Each time point was done in sextuplicate wells and experiments were repeated three times.

Colony-forming assay. Detailed experimental procedures have been described previously (3). Briefly, HepG2 cells stably transfected with shRNAs or empty vector were plated in 6-well plates at a density of 1,000 cells per well. After 10 days, cells

were washed with PBS, fixed in 10% methanol for 15 min, and stained in Giemsa for 20 min. Colonies that consisted of >50 cells were scored. Each experiment was repeated at least three times.

Cell cycle and apoptosis analysis. Cell cycle distribution was analyzed by flow cytometry as described previously (4). HepG2 and Hep3B cells stably transfected with shRNAs or empty vector were trypsinized, fixed in 70% ethanol, and incubated with 0.5 mg/ml of propidium iodide (PI) along with 0.1 mg/ml of RNase A (Calbiochem, San Diego, CA, USA). For apoptosis analysis, cells were stained with Annexin V/FITC kit (LHK601-100, MBI) in accordance with the manufacturer's instructions. Data acquisition and analysis were done using a FACSort Cytometer (FACSCA, New York, USA) with Multicycle software (Phoenix Flow Systems, San Diego, CA, USA). Experiments were replicated at least three times.

Quantitative reverse transcription-polymerase chain reaction (qRT-PCR). Total RNA was isolated using TRIzol (Invitrogen, Carlsbad, CA, USA) according to the manufacturer's instructions. The complementary DNA (cDNA) was reverse-transcribed from 2 μg of total RNA by SuperScript first-strand synthesis system for RT-PCR (Invitrogen). Real-time qPCR was performed on an ABI-7500 Sequence Detection System (Applied Biosystems, Foster City, CA, USA) using SYBR Green PCR Master Mix (Life Technologies Corporation, Foster City, CA, USA). Primer sequences used in this study included *MAP4K4* forward:

5'-ACAGAGAGTGGCCTGATGCT-3', *MAP4K4* reverse: 5'-ATC CTT CCA AAT CCC CTA CG-3'; and *β-actin* forward: 5'-GAG CGG GAA ATC GTG CGT GAC ATT-3', *β-actin* reverse: 5'-GAT GGA GTT GAA GGT AGT TTC GTG-3'. All samples were run in triplicate. Gene expression was normalized to the housekeeping gene β-actin transcripts, and the relative mRNA expression between the non-tumor and tumor samples were calculated using the $2^{-\Delta\Delta Ct}$ method (5).

***Antibodies and Western blot analysis*.** Western blotting was performed as described in ref. 6. Primary antibodies included anti-MAP4K4 (HGK, sc-25738; 1:500), anti-p-p38 (Thr 180, sc-101759; 1:500), anti-p38α (N-20, sc-728; 1:500), anti-p-ERK1/2 (Thr 202, sc-101760; 1:500) , anti-ERK1/2 (C-14, sc-154; 1:500), anti-p-JNK (G-7, sc-6254; 1:500), anti-JNK (D-2, sc-7345; 1:500), anti-p-NFκB p65 (Ser 276, sc-101749; 1:500), anti-NFκB p65 (F-6, sc-8008; 1:500), anti-TLR5 (H-127, sc-10742; 1:500), anti-TLR4 (H-80, sc-10741; 1:500), anti-MyD88 (HFL-296, sc-11356; 1:500), anti-TRAF6 (D-10, sc-8409; 1:500), and anti-β-actin (C4, sc-47778; 1:500). Equal amounts of protein (50 μg) was loaded, separated by sodium dodecyl sulfate-polyacrylamide gel electrophoresis (SDS-PAGE), and transferred onto polyvinylidene difluoride membranes. After blocking, the membranes were probed with primary antibody overnight at 4°C, followed by incubation with appropriate secondary antibody for 1 h. All antibodies were obtained from Santa Cruz Biotechnology. Blots were developed using an enhanced chemiluminescence kit from Santa Cruz Biotechnology. The intensities of immunoreactive bands were measured

by computerized image analysis (QuantityOne-software, Bio-Rad, Hercules, CA, USA) and normalized to β-actin levels.

Immunohistochemistry. Immunohistochemical staining for MAP4K4 was performed as described earlier (7). Briefly, paraffin sections (4 μm thick) were deparaffinized with xylene, rehydrated, and heated for 10 min in a steamer containing 10 mmol/L of sodium citrate (pH 6.0) to retrieve antigen. Endogenous peroxidase was quenched with 3% hydrogen peroxide for 10 min. Sections were incubated with rabbit polyclonal anti-MAP4K4 (HGK, sc-25738; 1:50) for 1 h, followed by the secondary reaction with DAKO Envision+ Reagent (DakoCytomation, Carpinteria, CA, USA). Negative controls were included by omitting the primary antibody, and a known positive control was included with each batch. The stained sections were independently assessed by two pathologists without prior knowledge of the clinical data. The mean percentage of immunoreactive cells in 5 representative areas of the slides was determined. Stained cells in most of the slides showed comparable immunoreactivity for MAP4K4 regardless of the percentage of positive cells; therefore, we did not take the intensity of staining into account. In accordance with the methods reported previously (7), the median percentage of immunostained tumor cells (10%) was used as a cutoff. High expression of MAP4K4 (MAP4K4-H) was defined as cytoplasmic staining of ≥10% of the tumor cells and low expression of MAP4K4 (MAP4K4-L) was defined as cytoplasmic staining of <10% of the tumor cells or no cytoplasmic staining. Association between MAP4K4 expression and

clinicopathological parameters were then analyzed.

1. Tuschl T. Expanding small RNA interference. Nat Biotechnol 2002;20:446-448.

2. Carmichael J, Mitchell JB, DeGraff WG, et al. Chemosensitivity testing of human lung cancer cell lines using the MTT assay. Br J Cancer 1988;57:540-547.

3. Wang X, Jin DY, Wong HL, Feng H, Wong YC, Tsao SW. MAD2-induced sensitization to vincristine is associated with mitotic arrest and Raf/Bcl-2 phosphorylation in nasopharyngeal carcinoma cells. Oncogene 2003;22:109-116.

4. Zhu Z, Luo Z, Li Y, Ni C, Li H, Zhu M. Human inhibitor of growth 1 inhibits hepatoma cell growth and influences p53 stability in a variant-dependent manner. Hepatology 2009;49:504-512.

5. Livak KJ, Schmittgen TD. Analysis of relative gene expression data using real-time quantitative PCR and the 2(-Delta Delta C(T)) Method. Methods 2001;25:402-408.

6. Collins CS, Hong J, Sapinoso L, et al. A small interfering RNA screen for modulators of tumor cell motility identifies MAP4K4 as a promigratory kinase. Proc Natl Acad Sci U S A 2006;103:3775-3780.

7. Liang JJ, Wang H, Rashid A, et al. Expression of MAP4K4 is associated with worse prognosis in patients with stage II pancreatic ductal adenocarcinoma. Clin Cancer Res 2008;14:7043-7049.

Supplementary Table 1. Clinicopathologic factors of two cohorts of patients with pathologically diagnosed HCC

Variables	Cohort A (n=20), no. cases	Cohort B (n=400), no. cases
Sex (male/female)	14/6	286/114
Median (range) age, y	51 (29-76)	50 (27-78)
Serum AFP level (≥20/<20 μg/l)	13/7	263/137
Serum HBsAg (positive/negative)	14/6	305/95
Serum HBeAg (positive/negative)	12/8	245/155
Tumor size (>2/≤2 cm)	16/4	343/57
Histological grade (well/moderate/poor)	3/10/7	95/236/69
Liver cirrhosis (absent/present)	13/7	125/275
Tumor capsule (intact/absent, not intact)	4/16	79/321
Intrahepatic metastasis (absent/present)	5/15	126/247
TNM stage (I + II/III + IV)	3/17	85/315

Supplementary Table 2. Genes on human TLR signaling pathway PCR arrays whose expression is regulated by MAP4K4 silencing in HepG2 cells

Position	GenBank no.	Symbol	Description	Gene name	Fold change (MAP4K4-A1/control shRNA transfectants)			
					Sample 1/ control 1	Sample 2/ control 2	Sample 3/ control 3	mean±Standard deviation
A01	NM_000061	BTK	Bruton agammaglobulinemia tyrosine kinase	AGMX1/AT	-1.87	-1.74	-1.66	-1.76±0.11
A02	NM_001228	CASP8	Caspase 8, apoptosis-related cysteine peptidase	ALPS2B/CAP4	-1.01	-1.61	-1.01	-1.21±0.35
A03	NM_002982	CCL2	Chemokine (C-C motif) ligand 2	GDCF-2/GDCF-2 HC11	-12.43	-18.15	-14.3	-14.96±2.93
A04	NM_000591	CD14	CD14 molecule	CD14	-2.29	-2.03	-2.15	-2.16±0.13
A05	NM_005191	CD80	CD80 molecule	CD28LG/CD28LG1	1.85	1.64	1.34	1.61±0.26
A06	NM_006889	CD86	CD86 molecule	B7-2/B70	-1.31	-1.2	-1.03	-1.18±0.14
A07	NM_001278	CHUK	Conserved helix-loop-helix ubiquitous kinase	IKBKA/IKK-alpha	-3.21	-5.29	-4.80	-4.43±1.09
A08	NM_014358	CLEC4E	C-type lectin domain family 4, member E	CLECSF9/MINCLE	-3.13	-4.50	-3.80	-3.89±0.81
A09	NM_000758	CSF2	Colony stimulating factor 2 (granulocyte-macrophage)	GMCSF	-3.82	-2.71	-3.08	-3.20±0.57
A10	NM_000759	CSF3	Colony stimulating factor 3 (granulocyte)	G-CSF/GCSF	-2.03	-1.99	-2.03	-2.02±0.02

A11	NM_001565	CXCL10	Chemokine (C-X-C motif) ligand 10	C7/IFI10	-3.66	-5.09	-4.74	-4.50±0.75
A12	NM_002759	EIF2AK2	Eukaryotic translation initiation factor 2-alpha kinase 2	EIF2AK1/PKR	-1.05	-1.87	-1.14	-1.35±0.45
B01	NM_005229	ELK1	ELK1, member of ETS oncogene family	Elk1	-4.45	-6.92	-5.31	-5.56±1.25
B02	NM_003824	FADD	Fas (TNFRSF6)-associated via death domain	GIG3/MORT1	-1.32	-1.04	-1.04	-1.13±0.16
B03	NM_005252	FOS	V-fos FBJ murine osteosarcoma viral oncogene homolog	c-fos	-5.19	-4.59	-4.07	-4.61±0.56
B04	NM_002128	HMGB1	High-mobility group box 1	DKFZp686A04236/ HMG1	-5.55	-6.4	-6.82	-6.26±0.55
B05	NM_005343	HRAS	V-Ha-ras Harvey rat sarcoma viral oncogene homolog	CTLO/HRAS1	-1.11	-1.75	-1.66	-1.51±0.35
B06	NM_005345	HSPA1A	Heat shock 70kDa protein 1A	HSP70-1/HSP72	4.99	4.82	4.13	4.65±0.46
B07	NM_002156	HSPD1	Heat shock 60kDa protein 1 (chaperonin)	CPN60/GROEL	-1.49	-1.28	-1.33	-1.37±0.11
B08	NM_024013	IFNA1	Interferon, alpha 1	IFL/IFN	-2.76	-2.83	-2.63	-2.74±0.10
B09	NM_002176	IFNB1	Interferon, beta 1, fibroblast	IFB/IFF	-3.61	-2.31	-3.28	-3.07±0.68
B10	NM_000619	IFNG	Interferon, gamma	IFG/IFI	-1.30	-1.18	-1.03	-1.17±0.14
B11	NM_001556	IKBKB	Inhibitor of kappa light polypeptide gene enhancer in B-cells, kinase beta	IKK-beta/IKK2	-1.85	-3.13	-2.01	-2.33±0.70
B12	NM_000572	IL10	Interleukin 10	CSIF/IL-10	-1.86	-1.03	-1.24	-1.38±0.43
C01	NM_000882	IL12A	Interleukin 12A (natural killer cell stimulatory factor 1, cytotoxic	CLMF/IL-12A	-2.84	-3.86	-3.44	-3.38±0.51

			lymphocyte maturation factor 1, p35)					
C02	NM_000575	IL1A	Interleukin 1, alpha	IL-1A/IL1	-6.63	-4.87	-6.84	-6.11±1.08
C03	NM_000576	IL1B	Interleukin 1, beta	IL-1/IL1-BETA	-1.88	-1.45	-1.92	-1.75±0.26
C04	NM_000586	IL2	Interleukin 2	IL-2/TCGF	-2.46	-1.05	-1.03	-1.51±0.82
C05	NM_000600	IL6	Interleukin 6 (interferon, beta 2)	BSF2/HGF	-1.06	-2.45	-2.66	-2.06±0.87
C06	NM_000584	IL8	Interleukin 8	3-10C/AMCF-I	-2.30	-1.70	-2.11	-2.04±0.31
C07	NM_001569	IRAK1	Interleukin-1 receptor-associated kinase 1	IRAK/pelle	-7.54	-8.66	-8.71	-8.30±0.66
C08	NM_001570	IRAK2	Interleukin-1 receptor-associated kinase 2	IRAK-2	-4.59	-2.92	-3.96	-3.82±0.84
C09	NM_002198	IRF1	Interferon regulatory factor 1	IRF-1/MAR	-1.08	-1.26	-1.65	-1.33±0.29
C10	NM_001571	IRF3	Interferon regulatory factor 3	IRF-3	-2.08	-2.95	-2.42	-2.48±0.44
C11	NM_002228	JUN	Jun oncogene	AP1/c-Jun	-1.12	-1.61	-1.65	-1.46±0.30
C12	NM_000595	LTA	Lymphotoxin alpha (TNF superfamily, member 1)	LT/TNFB	-1.69	-4.46	-2.75	-2.97±1.40
D01	NM_005582	CD180	CD180 molecule	LY64/Ly78	-1.12	-1.32	-1.5	-1.31±0.19
D02	NM_004271	LY86	Lymphocyte antigen 86	MD-1/MMD-1	-1.24	-1.33	-1.03	-1.20±0.15
D03	NM_015364	LY96	Lymphocyte antigen 96	MD-2	-3.33	-5.71	-4.94	-4.66±1.21
D04	NM_002756	MAP2K3	Mitogen-activated protein kinase kinase 3	MAPKK3/MEK3	1.81	1.78	1.61	1.74±0.11
D05	NM_003010	MAP2K4	Mitogen-activated protein kinase kinase 4	JNKK/JNKK1	-5.67	-4.70	-5.10	-5.16±0.49
D06	NM_005921	MAP3K1	Mitogen-activated protein kinase kinase kinase 1	MAPKKK1/MEKK	-36.8	-43.6	-40.45	-40.28±3.40
D07	NM_003188	MAP3K7	Mitogen-activated protein kinase	TAK1/TGF1a	-2.24	-2.66	-2.66	-2.52±0.24

			kinase kinase 7					
D08	NM_006116	MAP3K7IP1	Mitogen-activated protein kinase kinase kinase 7 interacting protein 1	3'-Tab1/TAB1	-3.48	-2.69	-3.28	-3.15±0.41
D09	NM_004834	MAP4K4	Mitogen-activated protein kinase kinase kinase kinase 4	FLH21957/HGK	-1.04	-1.47	-1.99	-1.50±0.48
D10	NM_002750	MAPK8	Mitogen-activated protein kinase 8	JNK/JNK1	-10.57	-16.54	-18.66	-15.26±4.19
D11	NM_015133	MAPK8IP3	Mitogen-activated protein kinase 8 interacting protein 3	DKFZp762N1113/JIP3	-2.2	-2.28	-2.02	-2.17±0.13
D12	NM_002468	MYD88	Myeloid differentiation primary response gene (88)	MyD88	-14.82	-12.91	-14.5	-14.08±1.02
E01	NM_003998	NFKB1	Nuclear factor of kappa light polypeptide gene enhancer in B-cells 1 (p105)	DKFZp686C01211/ EBP-1	-2.36	-3.49	-2.97	-2.94±0.57
E02	NM_002502	NFKB2	Nuclear factor of kappa light polypeptide gene enhancer in B-cells 2 (p49/p100)	LYT-10/LYT10	-1.02	-3.13	-2.2	-2.12±1.06
E03	NM_020529	NFKBIA	Nuclear factor of kappa light polypeptide gene enhancer in B-cells inhibitor, alpha	IKBA/MAD-3	-1.1	-2.02	-1.72	-1.61±0.47
E04	NM_005007	NFKBIL1	Nuclear factor of kappa light polypeptide gene enhancer in B-cells inhibitor-like 1	IKBL/LST1	-5.9	-4.62	-4.31	-4.94±0.84
E05	NM_006165	NFRKB	Nuclear factor related to kappaB binding protein	DKFZp547B2013	-4.69	-4.21	-4.18	-4.36±0.29
E06	NM_003298	NR2C2	Nuclear receptor subfamily 2, group C, member 2	TAK1/TR2R1	-3.99	-3.98	-4.35	-4.11±0.21

E07	NM_020651	PELI1	Pellino homolog 1 (Drosophila)	DKFZp686C18116	-2.96	-3.74	-3.71	-3.47±0.44
E08	NM_005036	PPARA	Peroxisome proliferative activated receptor, alpha	NR1C1/PPAR	-3.18	-3.56	-3.93	-3.55±0.37
E09	NM_003690	PRKRA	Protein kinase, interferon-inducible double stranded RNA dependent activator	HSD14/PACT	-4.22	-3.08	-3.24	-3.51±0.62
E10	NM_000963	PTGS2	Prostaglandin-endoperoxide synthase 2 (prostaglandin G/H synthase and cyclooxygenase)	COX-2/COX2	1.09	-1.03	-1.03	-0.32±1.22
E11	NM_002908	REL	V-rel reticuloendotheliosis viral oncogene homolog (avian)	C-Rel	-3.95	-3.14	-3.09	-3.39±0.48
E12	NM_021975	RELA	V-rel reticuloendotheliosis viral oncogene homolog A, nuclear factor of kappa light polypeptide gene enhancer in B-cells 3, p65 (avian)	NFKB3	-2.75	-2.32	-2.75	-2.61±0.25
F01	NM_003821	RIPK2	Receptor-interacting serine-threonine kinase 2	CARD3/CARDIAK	-5.62	-3.27	-4.58	-4.49±1.18
F02	NM_015077	SARM1	Sterile alpha and TIR motif containing 1	SAMD2/SARM	-1.90	-1.68	-1.56	-1.71±0.17
F03	NM_021805	SIGIRR	Single immunoglobulin and toll-interleukin 1 receptor (TIR) domain	TIR8	-1.28	-1.09	-1.24	-1.20±0.10
F04	NM_016581	ECSIT	ECSIT homolog (Drosophila)	SITPEC	-2.46	-4.10	-3.54	-3.37±0.84
F05	NM_013254	TBK1	TANK-binding kinase 1	NAK/T2K	-3.74	-2.55	-3.17	-3.15±0.76
F06	NM_021649	TICAM2	Toll-like receptor adaptor molecule 2	TICAM-2/TIRAP3	1.89	1.73	1.81	1.81±0.08

F07	NM_001039661	TIRAP	Toll-interleukin 1 receptor (TIR) domain containing adaptor protein	Mal/wyatt	-1.48	-1.08	-1.14	-1.23±0.22
F08	NM_003263	TLR1	Toll-like receptor 1	CD281/DKFZp547I0610	1.88	1.86	1.29	1.68±0.34
F09	NM_030956	TLR10	Toll-like receptor 10	CD290	-5.80	-9.13	-6.52	-7.15±1.75
F10	NM_003264	TLR2	Toll-like receptor 2	CD282/TIL4	1.51	1.19	1.08	1.26±0.22
F11	NM_003265	TLR3	Toll-like receptor 3	CD283	-2.15	-5.27	-3.77	-3.73±1.56
F12	NM_138554	TLR4	Toll-like receptor 4	ARMD10/CD284	-18.26	-23.57	-19.48	-20.44±2.78
G01	NM_003268	TLR5	Toll-like receptor 5	SLEB1/TIL3	-61.89	-37.65	-51.04	-50.19±12.14
G02	NM_006068	TLR6	Toll-like receptor 6	CD286	-2.18	-1.84	-2.64	-2.22±0.40
G03	NM_016562	TLR7	Toll-like receptor 7	TLR7	-3.50	-19.04	-10.2	-10.91±7.79
G04	NM_138636	TLR8	Toll-like receptor 8	CD288	-8.03	-6.78	-9.72	-8.18±1.48
G05	NM_017442	TLR9	Toll-like receptor 9	CD289	-1.22	-1.31	-1.03	-1.19±0.14
G06	NM_000594	TNF	Tumor necrosis factor (TNF superfamily, member 2)	DIF/TNF-alpha	1.92	1.10	1.09	1.37±0.48
G07	NM_001065	TNFRSF1A	Tumor necrosis factor receptor superfamily, member 1A	CD120a/FPF	1.02	-1.08	-1.03	-0.36±1.20
G08	NM_019009	TOLLIP	Toll interacting protein	IL-1RAcPIP	-1.26	-3.84	-2.08	-2.39±1.32
G09	NM_004620	TRAF6	TNF receptor-associated factor 6	MGC:3310/RNF85	-3.16	-2.18	-2.47	-2.60±0.50
G10	NM_182919	TICAM1	Toll-like receptor adaptor molecule 1	PRVTIRB/TICAM-1	-4.72	-2.67	-3.24	-3.54±1.06
G11	NM_003348	UBE2N	Ubiquitin-conjugating enzyme E2N (UBC13 homolog, yeast)	UBC13/UbcH-ben	-8.63	-3.8	-6.43	-6.29±2.42
G12	NM_021988	UBE2V1	Ubiquitin-conjugating enzyme E2 variant 1	CIR1/CROC-1	-1.44	-2.48	-1.64	-1.85±0.55
H01	NM_004048	B2M	Beta-2-microglobulin	B2M	-4.61	-2.98	-3.51	-3.70±0.83

H02	NM_000194	HPRT1	Hypoxanthine phosphoribosyltransferase 1 (Lesch-Nyhan syndrome)	HGPRT/HPRT	-1.08	-1.57	-1.40	-1.35±0.25
H03	NM_012423	RPL13A	Ribosomal protein L13a	RPL13A	-1.14	-1.72	-1.65	-1.50±0.32
H04	NM_002046	GAPDH	Glyceraldehyde-3-phosphate dehydrogenase	G3PD/GAPD	-1.34	-1.15	-1.03	-1.17±0.16
H05	NM_001101	ACTB	Actin, beta	PS1TP5BP1	1.45	1.80	1.45	1.57±0.20

Supplementary Table 3. Effects of MAP4K4 downregulation on cell cycle distribution and apoptotic index in HepG2 cells stably expressing indicated shRNAs

Groups	G0-G1 (%)	S phase (%)	G2/M (%)	Apoptotic index (%)
Control shRNA	58.87±5.34	28.75±3.41	12.38±1.92	4.557±0.79
MAP4K4-A1	20.16±2.65**	61.06±0.95**	18.78±3.59*	22.46±2.73**
MAP4K4-A2	59.30±3.68	22.38±6.68	18.31±3.01*	5.470±0.77
MAP4K4-A3	41.07±3.82**	43.48±1.72**	15.45±2.10	11.06±1.31*

NOTE: Values are presented as mean and SD of three independent experiments. *$P<0.05$, ** $P<0.01$, compared to the control shRNA-expressing transfectants.

Supplementary Table 4. Effects of MAP4K4 knockdown on gene expression in HepG2 cells

TLRs	Adaptors & TLR interacting proteins	Effectors	NFκB pathway	JNK/p38 pathway	NF/IL6 pathway	IRF pathway	Regulation of adaptive immunity	Fold change
TLR5	MyD88		CCL2	MAP3K1				>10, ↓
TLR4				MAPK8				
TLR7								
TLR8	HMGB1	IRAK1	IL1A	ELK1				>5, ↓
TLR10		UBE2N		MAP2K4				
	LY96	NR2C2	CHUK	FOS		CXCL10	RIPK2	>4, ↓
			NFKBIL1					
			NFRKB					
TLR3	PELI1,	IRAK2	IL12A		CLECSF9	TBK1		>3, ↓
	TICAM2	PPARA	IFNB1					
		SITPEC	MAP3K7IP1					
		PPARA	REL					
			CSF2					
TLR6	CD14,	MAP3K7	NFKB1	MAPK8IP3	IRF3			>2, ↓
	TOLLIP	TRAF6	RELA					
			LTA					
			IL-6					
			IFNA1					
			NFKB2					
			IL-8					
			CSF3					
			IKBKB					
			MAP4K4					
	HSPA1A							>2, ↑

NOTE: Fold difference in gene expression between HepG2 transfectants expressing MAP4K4-A1 and control shRNA. Average results of three independent experiments are shown, *n*=3. The genes listed are those whose expression is changed at least 2-fold. ↑,upregulation; ↓, downregulation, relative to the control transfectants.